

Energy & Environmental Science

Accepted Manuscript



This is an *Accepted Manuscript*, which has been through the Royal Society of Chemistry peer review process and has been accepted for publication.

Accepted Manuscripts are published online shortly after acceptance, before technical editing, formatting and proof reading. Using this free service, authors can make their results available to the community, in citable form, before we publish the edited article. We will replace this *Accepted Manuscript* with the edited and formatted *Advance Article* as soon as it is available.

You can find more information about *Accepted Manuscripts* in the [Information for Authors](#).

Please note that technical editing may introduce minor changes to the text and/or graphics, which may alter content. The journal's standard [Terms & Conditions](#) and the [Ethical guidelines](#) still apply. In no event shall the Royal Society of Chemistry be held responsible for any errors or omissions in this *Accepted Manuscript* or any consequences arising from the use of any information it contains.



Journal Name

ARTICLE

Sunlight-activated graphene-heterostructure transparent cathodes: enabling high-performance *n*-graphene/*p*-Si Schottky junction photovoltaics

Received 00th January 20xx,
Accepted 00th January 20xx

DOI: 10.1039/x0xx00000x

www.rsc.org/

^aPo-Hsun Ho, ^aWei-Chen Lee, ^aYi-Ting Liou, ^bYa-Ping Chiu, ^{a,c}Yi-Siang Shih, ^aChun-Chi Chen, ^aPao-Yun Su, ^aMin-Ken Li, ^aHsuen-Li Chen, ^cChi-Te Liang, ^{a,d,*}Chun-Wei Chen

Compared to widely-reported graphene-based anode, the task to obtain a stable graphene-based cathode is generally more difficult to achieve because *n*-type graphene devices have very limited thermal and chemical stabilities, and are usually sensitive to the influence of ambient environment. This work developed a novel “sunlight-activated” graphene-heterostructure transparent electrode in which photogenerated charges from a light-absorbing material are transferred to graphene, resulting in the modulation of electrical properties of the graphene electrode caused by a strong light–matter interaction at graphene-heterostructure interfaces. A photoactive graphene/TiO_x-heterostructure transparent cathode was used to fabricate an *n*-graphene/*p*-Si Schottky junction solar cell, achieving a record-high power conversion efficiency (>10%). The photoactive graphene-heterostructure transparent electrode, which exhibits excellent tunable electrical properties under sunlight illumination, has great potential for use in the future development of graphene-based photovoltaics and optoelectronics.

Introduction

Graphene exhibits excellent carrier transport because of its unique two-dimensional energy dispersion. In addition, a single-layer graphene shows high transparency with 97.7% transmittance,^{1,2} making it a candidate for transparent electrode applications with the potential to replace the conventional indium tin oxide (ITO). One advantage of using graphene as a transparent electrode compared to ITO is that graphene exhibits tunable electrical properties such as conductivity, work function, and carrier types (*n* or *p*) and concentrations that can be modulated through doping. Typically, the task to obtain a stable graphene-based cathode consisting of low work function and excellent conductivity is generally more difficult to achieve compared to widely-reported graphene-based anodes,^{3,4} because *n*-type graphene devices have very limited thermal and chemical stabilities, and are usually sensitive to the influence of ambient environment.⁵

Recently, significant progress in *p*-graphene/*n*-Si Schottky junction solar cells in which graphene functions as an anode has been demonstrated, achieving promising efficiencies of

10%–14%.^{6–9} By contrast, the performance of *n*-graphene/*p*-Si Schottky junction solar cell in which graphene functions as a cathode is still quite low, showing an efficiency of <0.1%^{10,11} because of the difficulty in obtaining an effective *n*-graphene transparent cathode with a suitable doping level and appropriate interface with *p*-Si. Most researchers have fabricated graphene transparent electrodes with tunable electrical properties using chemical doping by either incorporating substitutional dopants into carbon lattices or adsorbing surface charge dopants such as organic molecules,^{12–15} inorganic nanoparticles,^{16,17} and thin films^{18,19} on a graphene surface. Here, we would like to demonstrate a new concept of a “photoactive” graphene-heterostructure transparent electrode in which photogenerated charges from a light-absorbing material are transferred to graphene, resulting in the modulation of electrical properties of the electrode caused by a strong light–matter interaction at graphene-heterostructure interfaces. The photoactive graphene-heterostructure transparent electrode is particularly interesting when its electrical properties can be directly modulated through sunlight illumination in photovoltaic applications, resulting in significant improvement in power conversion efficiencies. Strong light–matter interactions in graphene-based heterostructure devices have recently shown unique physical phenomena and device functionality, resulting in controllable *p*- or *n*-doping processes under light illumination.^{20–25} For example, photoinduced modulating doping in graphene/BN heterostructures, where the dopants were separated from the conducting channel, resulted in a controllable *n*-type transport behavior of graphene with the

^a Department of Materials Science and Engineering, National Taiwan University, Taipei 106, Taiwan

^b Department of Physics, National Taiwan Normal University, Taipei 116, Taiwan

^c Department of Physics, National Taiwan University, Taipei 106, Taiwan

^d Taiwan Consortium of Emergent Crystalline Materials (TCECM), Ministry of Science and Technology, Taiwan

† Electronic Supplementary Information (ESI) available: [details of any supplementary information available should be included here]. See DOI: 10.1039/x0xx00000x

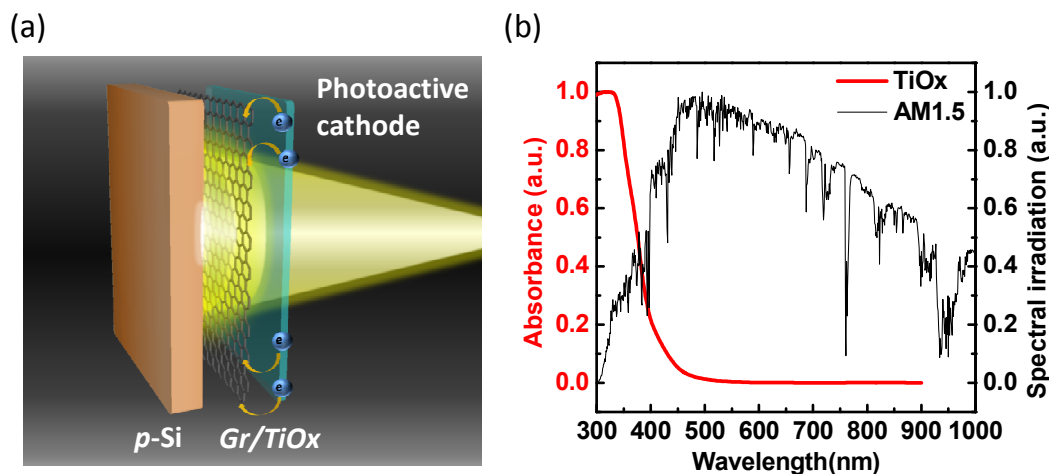


Fig. 1 (a) Schematic image of a TiOx/graphene/*p*-Si Schottky junction solar cell consisting of a graphene/TiOx heterostructure transparent cathode and a *p*-Si substrate. (b) Normalized absorption spectrum of the TiOx thin film (red) and solar irradiation spectrum under A.M. 1.5 illumination conditions (black).

preservation of high mobility under light illumination.²³ A hybrid graphene-PbS^{21,22} quantum dot device exhibited *p*-type transport behavior when the optically excited holes in quantum dots were transferred to graphene, yielding an ultrahigh photodetection gain.²² In addition, a graphene/WS₂/graphene van der Waals heterostructure showed a promising photovoltaic effect with a high quantum efficiency because of the strong coupling between layered constituents.²⁶ Photoinduced doping of graphene under light illumination is advantageous because it is more controllable and reversible than chemical doping. In this work, a “sunlight-activated” graphene/TiOx heterostructure transparent cathode was proposed and used to fabricate a high-performed *n*-graphene/*p*-Si Schottky junction solar cell that achieved a record-high power conversion efficiency of >10% because of unique photo-induced charge transfer at graphene/TiOx heterostructure interfaces. The breakthrough of fabricating high-performance *n*-graphene/*p*-Si Schottky junction solar cells has a great impact in the development of graphene-based photovoltaics because graphene could be acting both as an anode or a cathode with tunable electrical properties and excellent stability.

Results and discussion

The TiOx/graphene/*p*-Si Schottky junction solar cell consists of a graphene/TiOx heterostructure transparent cathode that is formed by spin coating a thin TiOx layer on top of graphene, and a *p*-Si substrate for light harvesting is present underneath the graphene as shown in Fig. 1(a). Solution-processable inorganic TiOx thin films, which are amorphous and transparent with a large energy gap, have recently been used as an efficient electron-donating agent to fabricate stable *n*-type graphene transistors because of their inherent oxygen vacancies.^{19,27} The band gap values of TiOx were found to be stoichiometrically dependent on the compositions of O/Ti

ratios²⁸ (supporting information). Fig. 1(b) shows the normalized absorption spectrum of the TiOx (*x* = 1.9) thin film used in this study and the dark line is the solar irradiation spectrum under air mass 1.5 global (A.M. 1.5) conditions. When incident photon energies are higher than the band gap of TiOx at wavelengths shorter than 400 nm, photogenerated charges from the TiOx thin film are expected to transfer to graphene, resulting in photoinduced doping at the graphene/TiOx interface. The near-ultraviolet (UV) light absorption of the TiOx film ensures that most of the sunlight can be transmitted through the graphene/TiOx transparent electrode to the underneath *p*-Si substrate, resulting in efficient light harvesting. The spectral match between TiOx absorption and solar irradiation implies that the graphene/TiOx heterostructure film can act as an effective “photoactive” transparent electrode under sunlight illumination without sacrificing the light harvesting efficiency.

High-quality CVD graphene thin films were grown to fabricate graphene/TiOx heterostructure films for transistors and transparent electrodes. TiOx thin films were deposited through spin coating and had a smooth surface with a roughness of approximately 0.30 nm. Depending on whether a film was used as a top or a bottom transparent electrode, two possible configurations of graphene/TiOx heterostructure thin films are proposed: the first corresponds to the top configuration and consists of a graphene film covered with a thin TiOx layer (TiOx/graphene), and the second corresponds to the bottom configuration and consists of a graphene film transferred on a precoated TiOx thin film (graphene/TiOx). These two different configurations are applicable when they are used as the top or bottom electrodes of devices respectively. Fig. 2(a) shows the optical transmittances of the as-grown monolayer graphene and the monolayer graphene covered with a 20 nm TiOx thin film. The TiOx/graphene film shows a high transparency with an optical transmittance of approximately 96.0% at 550 nm, comparable to the as-grown

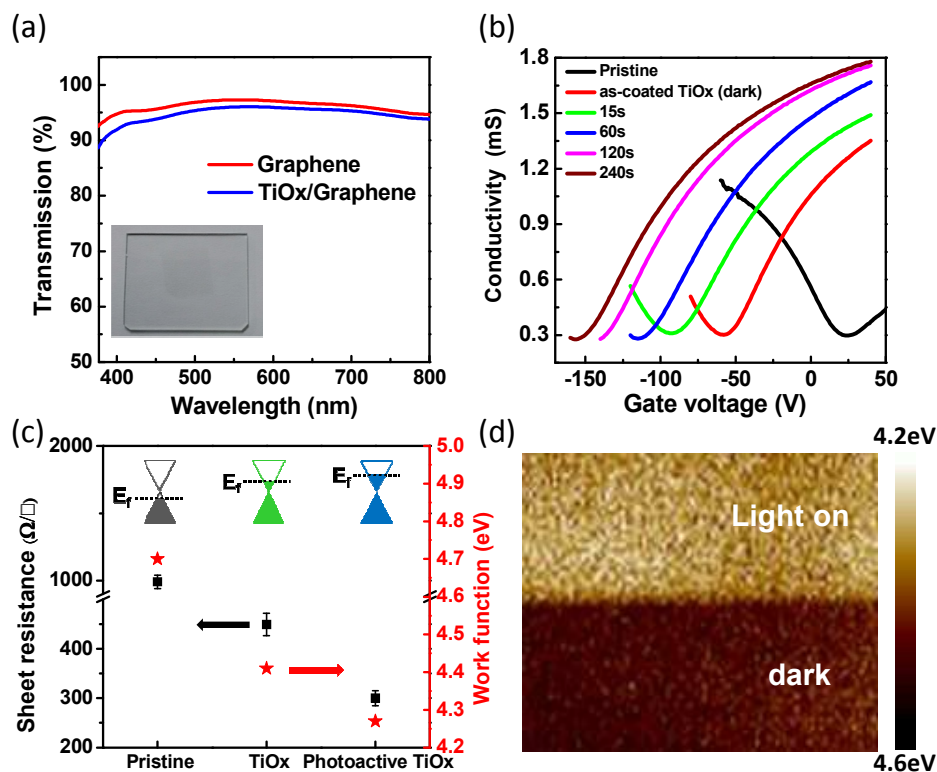


Fig. 2 (a) Transmission spectra of graphene and TiOx/graphene heterostructure films. (b) Gate-dependent current-voltage characteristics of a TiOx/graphene transistor under illumination (365nm, 10mW/cm²) with various illumination periods. (c) Sheet resistances of pristine graphene and graphene/TiOx heterostructure before and after illumination (black dot, left). The corresponding work function values measured by Kelvin probe force microscope are also shown in this figure. (red star, right) (d) Surface potential mapping images of a graphene/TiOx heterostructure film measured in the dark (bottom) and under light illumination (top).

monolayer graphene with a transmittance of approximately 97.3%. The inset of Fig. 2(a) shows the corresponding photographic image of the corresponding TiOx/graphene heterostructure transparent electrode transferred onto a glass substrate. To further investigate the photo-induced doping response in the TiOx/graphene heterostructure, a graphene transistor, which comprised a device structure of TiOx(20 nm)/graphene/SiO₂/Si by spin coating a TiOx thin film on top of graphene, was fabricated to measure its transport behavior under light illumination. Fig. 2(b) shows the gate-voltage (V_G)-dependent current of the device in the dark and under illumination. For comparison, an as-grown graphene transistor deposited on SiO₂/Si was fabricated, which exhibited a typical *p*-type transporting behavior with a positive Dirac point at 24 V because of the adsorption of oxygen or residual impurities during the transfer.^{29,30} After the TiOx layer was deposited on graphene, an intrinsic *n*-type doping effect on the graphene transistor with a negative Dirac point at -58 V was observed because of inherent oxygen deficiencies.¹⁹ In addition, the inherent oxygen deficiencies of a non-stoichiometric amorphous TiOx thin film typically act as effective hole-trapping centers in gap states.²⁵ When incident photon

energies are higher than the band gap of TiOx, photoexcited electron-hole pairs are generated; the holes are trapped in the gap states, and electrons in the conduction band (CB) of the TiOx film are transferred to graphene according to the band alignment.²⁵ The continual shift of the Dirac points toward negative V_G with an increase in the irradiation time indicated that electron concentrations in the graphene transistor increased with illumination by using a 365 nm light emitting diode (LED) (10 mW/cm²). These processes reached a saturated level with a Dirac point at approximately -156 V when the device was illuminated for over 5 min because the trapped states of the TiOx film were completely filled. The transistor device subjected to photoinduced doping also exhibited a long recovery time even when the illuminated light was switched off because of the trapped charge (supporting information).

Fig. 2(c) shows the sheet resistances and work functions of pristine graphene, graphene/TiOx, and graphene/TiOx under light illumination. Here, the bottom configuration of the graphene/TiOx heterostructure fabricated by transferring graphene to a precoated TiOx thin film (20 nm) on a glass substrate was used for measurement. Both the resistance and

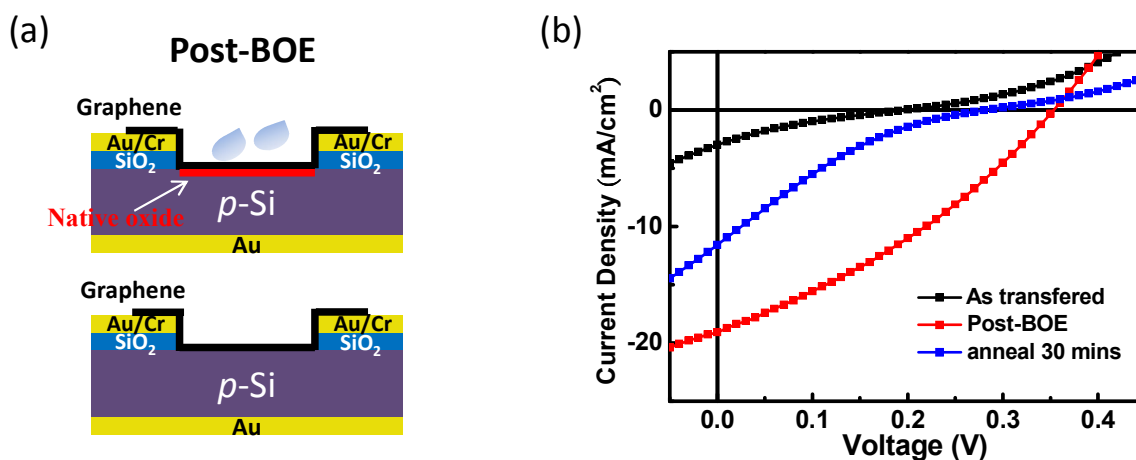


Fig. 3 (a) Schematic representation of a graphene/*p*-Si Schottky junction device with post-BOE treatment. (b) Current-voltage characteristics of a graphene/*p*-Si Schottky junction device before and after post-BOE treatment. The degradation of the device after annealing at ambient air for 30 min was also shown.

work function of the photoactive graphene/TiOx film were measured while the sample was under light illumination for >5 min (365 nm LED, 10 mW/cm²) to ensure that the photoinduced doping of the graphene/TiOx film reached a saturated level. The sheet resistances of the as-grown graphene, graphene/TiOx, and graphene/TiOx under light illumination were 900, 449, and 300 Ω/□ and the corresponding work functions measured by Kelvin probe force microscope were 4.70, 4.41, and 4.27 eV, respectively. The results show a good consistency with the observed trend of increasing carrier concentrations and a negative shift of Dirac points of the graphene transistor under light illumination (Fig. 2(b)). For the graphene/TiOx film without light illumination, the decreased sheet resistance and work function compared with those of pristine graphene is mainly attributed to intrinsic *n*-type doping by using the efficient electron-donating agent TiOx because of inherent oxygen vacancies.¹⁶ For the graphene/TiOx film under light illumination, the further decreased sheet resistance and work function are mainly attributed to photoinduced doping at the graphene/TiOx heterostructure, where photogenerated electrons in the CB of the TiOx film are transferred to graphene, resulting in an increased electron concentration and a raised Fermi level of graphene. Substantial photoinduced doping at the graphene/TiOx heterostructure is further evident from the work function mapping image, revealed using the scanning Kelvin probe force microscope, of graphene deposited on a TiOx thin film when it was measured in the dark and under light illumination. The decreased work function of the graphene/TiOx thin film under light illumination compared to that without illumination was clearly observed. (Fig. 2(d)) The remarkable photodoping response of the modulation of electrical properties of graphene caused by the near-UV absorption of TiOx suggests that the graphene/TiOx heterostructure transparent film has great potential for use in photovoltaic applications because it can simultaneously exhibit

strong photoinduced doping on graphene and preserve its high transparency in the visible–near infrared region under sunlight illumination.

Before we used the photoactive graphene/TiOx heterostructure transparent electrode in an *n*-graphene/*p*-Si Schottky junction solar cell, the formation of a native oxide layer at the interface between the graphene and the *p*-Si had to be addressed. For a graphene/Si Schottky junction, the formation of a thin native oxide between graphene and Si is usually inevitable. The interface between Si and SiO₂ usually consists of a large amount of hole traps, which are well-known in Si-based metal-oxide-semiconductor (MOS) device technology,^{31,32} and the interface traps at a native oxide layer greatly affect photocurrent transport. The influence of interface traps at the native oxide layer on the performance of an *n*-graphene/*p*-Si Schottky junction solar cell is found to be greater than that on a *p*-graphene/*n*-Si Schottky junction due to different directions of photocurrent in these two systems (supporting information). For the conventional fabrication of a graphene/Si device, a buffer oxide etchant (BOE) is usually used to remove the native oxide layer to obtain a fresh Si surface before graphene is transferred. However, because contamination of graphene with water or residual impurities during the transfer is usually inevitable, the native oxide layer between graphene and Si can grow further. Accordingly, we used a post-BOE treatment technique to eliminate the native oxide between graphene and Si by dropping a small amount of a BOE on the graphene/Si Schottky junction device (Fig. 3(a)). The BOE solution penetrated the defect sites of graphene and etched the native oxide layer between graphene and Si. The modified-BOE treatment could also be an effective method for removing oxygen contaminants on graphene³³ and carbon nanotubes,³⁴ which may result in *p*-type doping. Fig. 3(b) shows the current–voltage characteristics of the graphene/*p*-Si Schottky junction solar cells before and after the post-BOE treatment. The as-transferred graphene/*p*-Si Schottky junction

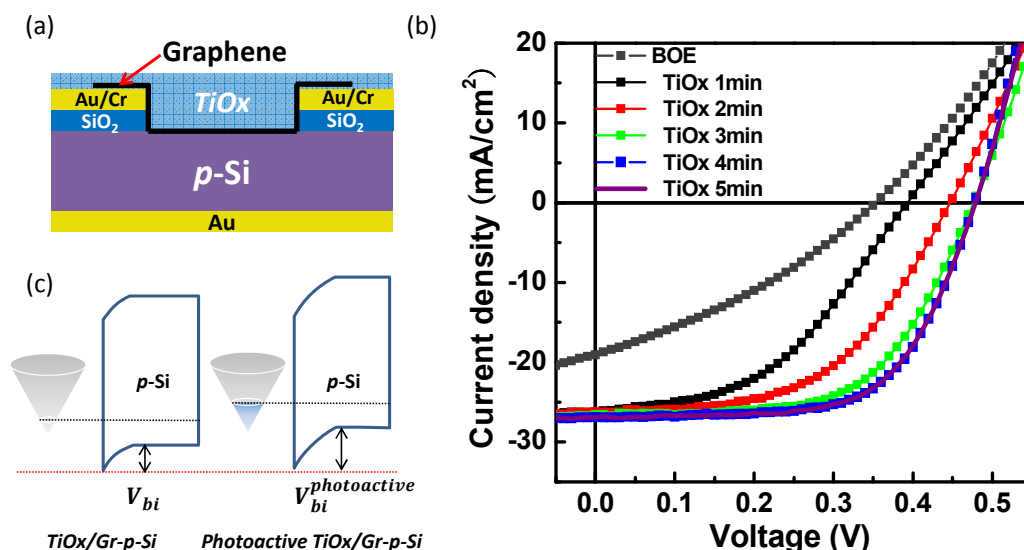


Fig. 4. (a) Schematic representation of a TiOx/graphene/Si Schottky junction solar cell. (b) Current-voltage characteristics of a TiOx/graphene/Si Schottky solar cell as a function of illumination time up to 5 min. The device reaches to a saturated performance after 4 min illumination. (c) The band diagrams of the built-potentials V_{bi} and $V_{bi}^{photoactive}$ of the TiOx/graphene/*p*-Si Schottky junction solar cells consisting of the as-deposited TiOx/graphene and photoactive TiOx/graphene cathodes.

solar cell without the post-BOE treatment exhibited a low power conversion efficiency of $\sim 0.1\%$, with an open circuit voltage (V_{OC}) of 0.20 V, a short circuit current (J_{SC}) of 2.98 mA/cm², and a fill factor (FF) of 0.169. By contrast, the device after post-BOE treatment exhibited a significant improvement in photovoltaic performance, showing a higher power conversion efficiency of 2.2% with V_{OC} of 0.35 V, J_{SC} of 19.1 mA/cm², and FF of 0.331. Therefore, removing the native oxide layer at the graphene/*p*-Si interface is a crucial factor for improving the device performance. However, the device showed a considerable degradation when it was annealed (150°C) under ambient conditions for 30 min, indicating that the native oxide layer grows further if the device is exposed to ambient air. The effect of the native oxide thickness on the device performance of a graphene/*p*-Si Schottky junction solar cell is shown in the supporting information. Therefore, an encapsulated layer that can prevent a device from degrading because of contamination with oxygen or water is necessary for extending the device stability. Because TiOx has been reported to be an effective encapsulated layer on graphene for preventing contamination with water and oxygen,¹⁹ the top TiOx layer of the TiOx/graphene/*p*-Si Schottky junction solar cell functions not only as an efficient photodoping material that modulates the electrical properties of graphene but also as an encapsulated layer that prevents the formation of a native oxide layer.

Fig. 4(a) shows the device structure of an *n*-graphene/*p*-Si Schottky junction solar cell that consists of the photoactive TiOx (20 nm)/graphene transparent cathode and the light-absorbing material *p*-Si. Fig. 4(b) shows the dynamic current-voltage characteristics of the TiOx/graphene/*p*-Si Schottky

junction solar cell under simulated A.M. 1.5 illumination (100 mW/cm²) for various measurement durations. For comparison, the performance of the referenced graphene/*p*-Si Schottky junction solar cell subjected to post-BOE treatment without coating of the TiOx layer is shown. The duration of measurement performed to obtain each current-voltage curve was maintained at approximately 1 min. The TiOx/graphene/*p*-Si Schottky junction solar cell device showed an intriguing phenomenon; a gradual enhancement in the power conversion efficiency as the illumination time increased was observed. According to the first measured current-voltage curve, the device showed an enhanced power conversion efficiency of 4.6% with V_{OC} of 0.40 V, J_{SC} of 26.2 mA/cm², and FF of 0.443. The device exhibited a continual increase in V_{OC} and FF when it was under illumination for up to 4 min, whereas there was no significant variation in J_{SC} . The power conversion efficiency of the TiOx/graphene/*p*-Si Schottky junction solar cell reached a saturated power conversion efficiency of 8.2% after 4 min of illumination, exhibiting V_{OC} of 0.48 V, J_{SC} of 26.9 mA/cm², and FF of 0.634. No further increase in the power conversion efficiency was observed when the device was illuminated for a longer time because the trapped states of TiOx were completely filled. The evolution of the power conversion efficiency of the TiOx/graphene/*p*-Si Schottky junction solar cell as the illumination time increased is also shown in Table 1. The promising value of 8.2% achieved by the *n*-graphene/*p*-Si Schottky junction solar cell indicates that the photoactive TiOx/graphene thin film functions as an effective transparent cathode, compared to that without coating the TiOx layer. The considerably enhanced power conversion efficiency and increased V_{OC} and FF of the TiOx/graphene/*p*-Si Schottky

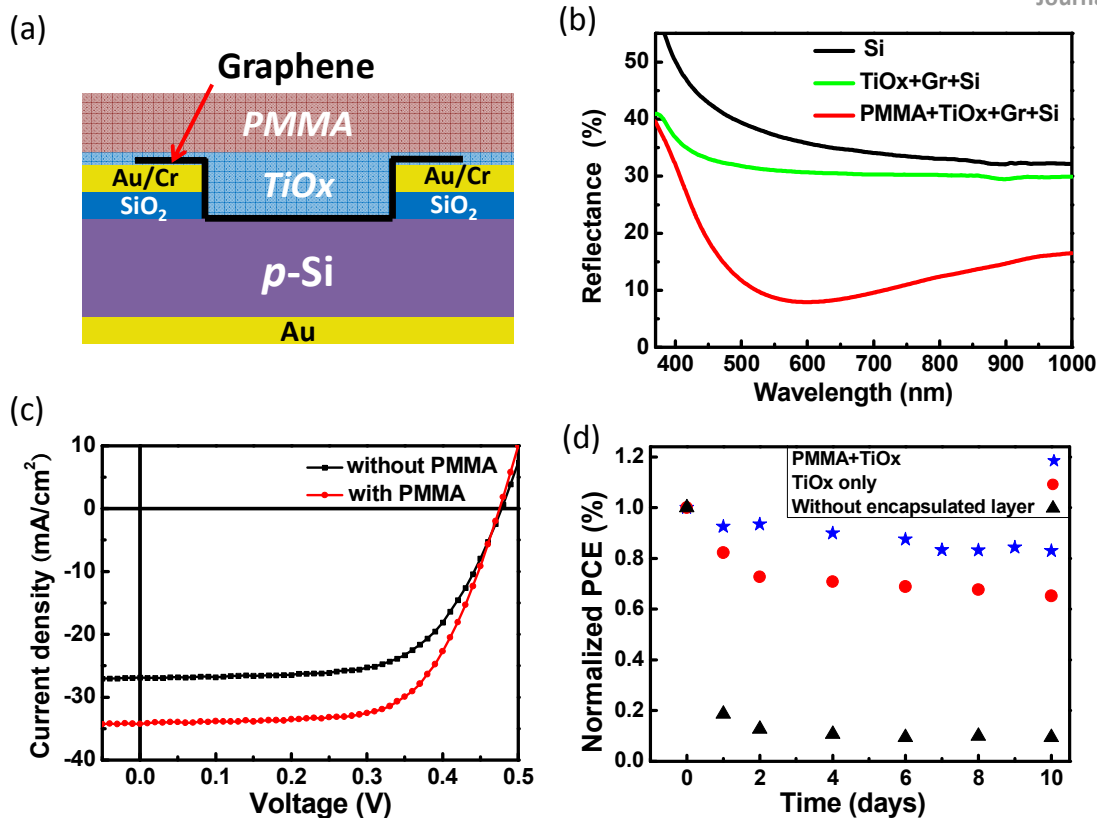


Fig. 5. (a) Schematic representation of a PMMA/TiOx/graphene/*p*-Si Schottky junction solar cell, where PMMA was used as an antireflective coating layer. (b) Reflection spectra of the pure *p*-Si, TiOx/graphene/*p*-Si, and PMMA/TiOx/graphene/*p*-Si. (c) The device performance of TiOx/graphene/*p*-Si Schottky junction solar cell with and without PMMA antireflective coating. (d) Stability test of the devices with and without an encapsulated layer when it was exposed to ambient air.

junction solar cell are mainly attributed to the unique photoinduced doping effect of the graphene/TiOx heterostructure under light illumination. First, the intrinsic *n*-type doping of the TiOx thin layer acts as an electron-donating agent, increasing the electron concentration and the Fermi level of graphene. In the TiOx/graphene/*p*-Si Schottky junction solar cell under sunlight illumination, substantial photoinduced doping results in the transfer of photoexcited electrons from TiOx to graphene as the TiOx thin layer absorbs near-UV light with wavelengths < 400 nm. At this stage, the electron concentrations and Fermi levels of graphene further increase because of photoinduced charge transfer at the graphene/TiOx interface, resulting in increased built-in voltages at the graphene/*p*-Si junction (Fig. 4(c)). The corresponding Schottky barrier heights of the TiOx/graphene/*p*-Si device were also found to be increased with illumination. (supporting information) This explains the systematic increase in the V_{oc} of the device when it was under simulated solar illumination. In addition, the improved FF of the device under illumination is mainly attributed to the increased carrier concentration of graphene, resulting in a decreased sheet resistance. Accordingly, the graphene/TiOx heterostructure thin film acts as a photoactive transparent cathode with tunable doping levels and work functions, enabling the *n*-graphene/*p*-Si

Schottky junction solar cell to achieve high performance as a result of unique photoinduced charge transfer at graphene/TiOx heterostructure interface.

Because a pristine Si substrate usually has a high reflectance (>30%), the device performance of the TiOx/graphene/*p*-Si Schottky junction solar cell could be further optimized by using an antireflection technique to enhance the light-trapping efficiency of the device. Polymethylmethacrylate (PMMA) was recently reported to be an effective antireflection material in carbon-based/Si Schottky junction solar cells.³⁵ Fig. 5(a) shows the device structure after an antireflection PMMA thin layer was deposited on the TiOx/graphene/*p*-Si Schottky junction solar cell. The optimized thickness of the PMMA layer was calculated to be approximately 70 nm using the Fresnel equation.(supporting information) Fig. 5(b) shows the reflection spectra (400–1100 nm) of the TiOx/graphene/*p*-Si Schottky junction solar cell before and after the PMMA antireflection layer was deposited. Before being coated with the PMMA layer, the TiOx/graphene/*p*-Si Schottky junction solar cell showed a slightly lower reflectance compared with that of a pristine Si substrate. After the PMMA layer was deposited on the TiOx/graphene/*p*-Si Schottky junction solar cell, the reflectance of the device was substantially reduced to

approximately 10% at 500–800 nm. The PMMA/TiOx/graphene/*p*-Si Schottky junction solar cell with the antireflection coating showed a high power conversion efficiency of 10.5% with V_{OC} of 0.48 V, J_{SC} of 34.3 mA/cm², and FF of 0.636 (Fig. 5(c)). The increased JSC of the device was mainly because of the increased light trapping efficiency achieved by using the antireflection technique. In addition, both PMMA and TiOx thin films are effective encapsulated layers that prevent the formation of a native oxide layer at the graphene/Si Schottky. Although TiOx is a good encapsulated layer which may prevent the device from being exposed to oxygen and water¹⁹, the thickness of TiOx is too thin to block all possible contamination in atmosphere. (supporting information) The device consisting of a double encapsulated layer (TiOx+PMMA) shows excellent air stability as demonstrated in Fig. 5(d). The device exhibited satisfactory stability, with >80% of the original power conversion efficiency after 10 day of exposure under ambient conditions.

Table 1. Photovoltaic parameters derived from J-V measurements of *n*-graphene/*p*-Si Schottky solar cell. The solar cell parameters of the devices are analyzed from Fig. 4(b) and Fig. 5(c). The detail photovoltaic parameters are open circuit voltage, V_{OC} , short circuit current, J_{SC} , fill factor, FF, and power conversion efficiency (PCE).

	V_{OC} (V)	J_{SC} (mA/cm ²)	FF (%)	PCE (%)
Post-BOE (Gr only)	0.35	19.1	32.6	2.2
TiOx/Gr 1min	0.40	26.2	44.3	4.6
TiOx/Gr 2min	0.45	26.4	51.6	6.1
TiOx/Gr 3min	0.47	26.6	60.2	7.5
TiOx/Gr 4min	0.48	26.9	63.4	8.2
PMMA/TiOx/Gr	0.48	34.3	63.6	10.5

Conclusion

In summary, we developed a novel photoactive graphene-heterostructure transparent electrode, where the carrier concentrations and work functions of graphene can be modulated through light illumination. The photoactive graphene transparent electrode is particularly unique in the photovoltaic application when sunlight acts as a modulating source on the electrical properties of graphene. The sunlight-activated graphene/TiOx heterostructure thin film acts as an effective graphene transparent cathode that enables the *n*-graphene/*p*-Si Schottky junction solar cells to exhibit high performance, achieving a record-high efficiency >10% for the first time. It is worth noting that although the power conversion efficiency of the *n*-graphene/*p*-Si Schottky junction

solar cell at current stage is still lower than those of *p*-graphene/*n*-Si Schottky junction solar cells (where graphene acts as an anode), the breakthrough of discovering the sunlight-activated graphene-heterostructure transparent cathodes can be also applied in other photovoltaic systems which require a stable graphene-based transparent cathode consisting of low work function and excellent conductivity. The self-encapsulated, sunlight-activated transparent electrode with tunable electrical properties under solar irradiation showed great potential for use in the development of graphene-based photovoltaics and optoelectronics.

Experimental

Chemical vapor deposition (CVD) was used for the growth of graphene on Cu foil.

A polycrystalline Cu foil (purchased from Sigma-Aldrich Inc.) was placed on a hot wall furnace consisting of a 1 inch fused silica tube. The furnace was then heated to 1000 °C. Typically, a reduction process was conducted in H₂ flow for ~40 min prior to the introduction of CH₄. With H₂ flow, CH₄ was then introduced for graphene growth with a flow rate of H₂/CH₄ of 2/35 sccm. After a growth time of 30 min, CH₄ was then shut off and the system was cooled in H₂ or Ar flow to reach room temperature. The whole procedures were conducted at low pressure (typically ~500 mtorr during the growth stage). The as-grown graphene films were transferred using the conventional PMMA transfer technique. TiOx was synthesized via sol-gel procedures according to our previous article.²⁸ For the bottom configuration of a graphene/TiOx heterostructure, the TiOx precursor solution was first spin-cast on substrate to form a thin film, followed by hydrolysis processes at 80°C. Subsequently, CVD-graphene film was transferred on the pre-coated TiOx substrate using the PMMA transferred method. For the top configuration of a TiOx/graphene heterostructure, the TiOx precursor was directly spin-cast on the as-transferred graphene film, followed by hydrolysis processes.

Fabrications of *n*-graphene/*p*-Si Schottky junction solar cells

A *p*-type silicon wafer (1~10Ωcm) with 300 nm thermal oxide was used for fabricating *n*-graphene/*p*-Si Schottky junction solar cells in this work. The Cr/Au contacts were defined at the front side of the Si wafer using the conventional photolithography technique. Subsequently, the backside of the SiO₂ layer was first removed by a buffered oxide etchant (BOE) with HF:NH₄F (1:6) to expose the surface of silicon, and then was evaporated with gold to form an ohmic contact at the backside of the Si wafer. The top patterned Cr/Au electrodes were utilized as masks for etching the front SiO₂ through the BOE process and the working area of the device is defined with an effective square window of 3 x3 mm². Subsequently, the as-grown graphene film was transferred through the PMMA method. The post-BOE treatment was taken by dropping the BOE on the working window for 3 min to etch the native oxide under graphene. Subsequently, a TiOx thin film was spin-cast on the device to fabricate a TiOx/graphene/*p*-Si Schottky

junction solar cell. For the antireflective coating, the PMMA (MicroChem 950 PMMA A6) diluted with chloroform (PMMA 20 vol% in chloroform) was spin-cast (8000 rpm) on the TiO_x/graphene/*p*-Si Schottky junction solar cell to form an antireflective and also an encapsulated layer.

Optical and Electrical Characterizations of devices

The transmission spectra were measured by a UV/Vis/NIR spectrophotometer (JASCO, V-570). Sheet resistances of graphene and CFG were characterized with Keithley 2400 source meter equipped with conventional four-probe station. The work function values of graphene samples were determined by using Kelvin probe force microscopy (KPFM) (Innova, Veeco Inc.). Current-voltage characteristics of the solar cell devices were measured by a Keithley 2410 source meter under an irradiation intensity of 100 mW/cm² from a solar simulator (Newport Inc.) with the A.M. 1.5 filter. The field-effect transistor was fabricated on heavily doped silicon wafer with thermally grown 300 nm silicon dioxide. After transferring graphene on the SiO₂/Si substrate, the source and drain electrodes (Au/Cr) were fabricated by utilizing thermal evaporation through a shadow mask with a channel length of 100 μm and a channel width of 1mm. The TiO_x was then spin-cast on top of the graphene transistor for further measurement. The optically illuminated gate-dependent conductivities of the device was measured (Keithley 6487 and 2410 for the source-drain and gate, respectively) in a probe station chamber (Linkam FDCS 196) at room temperature under a vacuum condition of 10⁻³ torr, coupled with a 365nm LED (Mightex). The optical reflectances of the *n*-graphene/*p*-Si photovoltaic devices were measured using a Hitachi U-4100 various-angle optical spectrometer.

Acknowledgements

This work is supported by Minster of Science and Technology (MOST), Taiwan (Project No. 103-2119-M-002 -021 -MY3 and 102-2119-M-002 -005) and Taiwan Consortium of Emergent Crystalline Materials (TCECM).

References

- 1 F. Bonaccorso, Z. Sun, T. Hasan and A. C. Ferrari, *Nat. Photon.*, 2010, **4**, 611-622.
- 2 Q. Bao and K. P. Loh, *ACS Nano*, 2012, **6**, 3677-3694.
- 3 H. Park, S. Chang, M. Smith, S. Gradecak and J. Kong, *Sci. Rep.*, 2013, **3**, 1581.
- 4 D. Zhang, F. Xie, P. Lin and W. C. H. Choy, *ACS Nano*, 2013, **7**, 1740-1747.
- 5 F. Schedin, A. K. Geim, S. V. Morozov, E. W. Hill, P. Blake, M. I. Katsnelson and K. S. Novoselov, *Nat. Mater.*, 2007, **6**, 652-655.
- 6 E. Shi, H. Li, L. Yang, L. Zhang, Z. Li, P. Li, Y. Shang, S. Wu, X. Li, J. Wei, K. Wang, H. Zhu, D. Wu, Y. Fang and A. Cao, *Nano Lett.*, 2013, **13**, 1776-1781.
- 7 C. Xie, X. Zhang, K. Ruan, Z. Shao, S. S. Dhaliwal, L. Wang, Q. Zhang, X. Zhang and J. Jie, *J. Mater. Chem. A*, 2013, **1**, 15348-15354.
- 8 K. Jiao, X. Wang, Y. Wang and Y. Chen, *J. Mater. Chem. C*, 2014, **2**, 7715-7721.
- 9 P.-H. Ho, Y.-T. Liou, C.-H. Chuang, S.-W. Lin, C.-Y. Tseng, D.-Y. Wang, C.-C. Chen, W.-Y. Hung, C.-Y. Wen and C.-W. Chen, *Adv. Mater.*, 2015, **27**, 1724-1729.
- 10 S. K. Behura, S. Nayak, I. Mukhopadhyay and O. Jani, *Carbon*, 2014, **67**, 766-774.
- 11 M. Mohammed, Z. Li, J. Cui and T.-p. Chen, *Nanoscale Res. Lett.*, 2012, **7**, 302.
- 12 D. B. Farmer, R. Golizadeh-Mojarad, V. Perebeinos, Y.-M. Lin, G. S. Tulevski, J. C. Tsang and P. Avouris, *Nano Lett.*, 2008, **9**, 388-392.
- 13 W. Chen, S. Chen, D. C. Qi, X. Y. Gao and A. T. S. Wee, *J. Am. Chem. Soc.*, 2007, **129**, 10418-10422.
- 14 P. Wei, N. Liu, H. R. Lee, E. Adijanto, L. Ci, B. D. Naab, J. Q. Zhong, J. Park, W. Chen, Y. Cui and Z. Bao, *Nano Lett.*, 2013, **13**, 1890-1897.
- 15 S. Tongay, K. Berke, M. Lemaitre, Z. Nasrollahi, D. B. Tanner, A. F. Hebard and B. R. Appleton, *Nanotechnology*, 2011, **22**, 425701.
- 16 K. K. Kim, A. Reina, Y. Shi, H. Park, L.-J. Li, Y. H. Lee and J. Kong, *Nanotechnology*, 2010, **21**, 285205.
- 17 X. Shi, G. Dong, M. Fang, F. Wang, H. Lin, W.-C. Yen, K. S. Chan, Y.-L. Chueh and J. C. Ho, *J. Mater. Chem. C*, 2014, **2**, 5417-5421.
- 18 I. Khrapach, F. Withers, T. H. Bointon, D. K. Polyushkin, W. L. Barnes, S. Russo and M. F. Craciun, *Adv. Mater.*, 2012, **24**, 2844-2849.
- 19 P.-H. Ho, Y.-C. Yeh, D.-Y. Wang, S.-S. Li, H.-A. Chen, Y.-H. Chung, C.-C. Lin, W.-H. Wang and C.-W. Chen, *ACS Nano*, 2012, **6**, 6215-6221.
- 20 S.-Y. Chen, Y.-Y. Lu, F.-Y. Shih, P.-H. Ho, Y.-F. Chen, C.-W. Chen, Y.-T. Chen and W.-H. Wang, *Carbon*, 2013, **63**, 23-29.
- 21 D. Zhang, L. Gan, Y. Cao, Q. Wang, L. Qi and X. Guo, *Adv. Mater.*, 2012, **24**, 2715-2720.
- 22 G. Konstantatos, M. Badioli, L. Gaudreau, J. Osmond, M. Bernechea, F. P. G. de Arquer, F. Gatti and F. H. L. Koppens, *Nat. Nanotechnol.*, 2012, **7**, 363-368.
- 23 JuL, J. Velasco Jr, HuangE, KahnS, NosigliaC, H.-Z. Tsai, YangW, TaniguchiT, WatanabeK, ZhangY, ZhangG, CrommieM, ZettlA and WangF, *Nat. Nanotechnol.*, 2014, **9**, 348-352.
- 24 W. Guo, S. Xu, Z. Wu, N. Wang, M. M. T. Loy and S. Du, *Small*, 2013, **9**, 3031-3036.
- 25 P.-H. Ho, S.-S. Li, Y.-T. Liou, C.-Y. Wen, Y.-H. Chung and C.-W. Chen, *Adv. Mater.*, 2015, **27**, 282-287.
- 26 L. Britnell, R. M. Ribeiro, A. Eckmann, R. Jalil, B. D. Belle, A. Mishchenko, Y.-J. Kim, R. V. Gorbachev, T. Georgiou, S. V. Morozov, A. N. Grigorenko, A. K. Geim, C. Casiraghi, A. H. C. Neto and K. S. Novoselov, *Science*, 2013, **340**, 1311-1314.
- 27 S. Cho, K. Lee and A. J. Heeger, *Adv. Mater.*, 2009, **21**, 1941-1944.
- 28 Y.-C. Yeh, S.-S. Li, C.-C. Wu, T.-W. Shao, P.-C. Kuo and C.-W. Chen, *Sol. Energ. Mat. Sol. C.*, 2014, **125**, 233-238.

- 29 S. Ryu, L. Liu, S. Berciaud, Y.-J. Yu, H. Liu, P. Kim, G. W. Flynn and L. E. Brus, *Nano Lett.*, 2010, **10**, 4944-4951.
- 30 X. Liang, B. A. Sperling, I. Calizo, G. Cheng, C. A. Hacker, Q. Zhang, Y. Obeng, K. Yan, H. Peng, Q. Li, X. Zhu, H. Yuan, A. R. Hight Walker, Z. Liu, L.-m. Peng and C. A. Richter, *ACS Nano*, 2011, **5**, 9144-9153.
- 31 L. Do Thanh and P. Balk, *J. Electrochem. Soc.*, 1988, **135**, 1797-1801.
- 32 P. M. Lenahan and P. V. Dressendorfer, *J. Appl. Phys.*, 1984, **55**, 3495-3499.
- 33 D.-W. Shin, H. M. Lee, S. M. Yu, K.-S. Lim, J. H. Jung, M.-K. Kim, S.-W. Kim, J.-H. Han, R. S. Ruoff and J.-B. Yoo, *ACS Nano*, 2012, **6**, 7781-7788.
- 34 X. Li, J.-S. Huang, S. Nejati, L. McMillon, S. Huang, C. O. Osuji, N. Hazari and A. D. Taylor, *Nano Lett.*, 2014, **14**, 6179-6184.
- 35 R. Li, J. Di, Z. Yong, B. Sun and Q. Li, *J. Mater. Chem. A*, 2014, **2**, 4140-4143.

Broader Context:

Typically, the task to obtain a stable graphene-based cathode consisting of low work function and excellent conductivity is generally more difficult to achieve compared to widely-reported graphene-based anodes, because n-type graphene devices have very limited thermal and chemical stabilities, and are usually sensitive to the influence of ambient environment. This work demonstrate a new concept of a “photoactive” graphene-heterostructure transparent electrode in which photogenerated charges from a light-absorbing material are transferred to graphene, resulting in the modulation of electrical properties of the electrode caused by a strong light–matter interaction at graphene-heterostructure interfaces. A “sunlight-activated” graphene/TiO_x heterostructure transparent cathode was proposed and used to fabricate a high-performed *n*-graphene/*p*-Si Schottky junction solar cell that achieved a record-high power conversion efficiency because of unique photo-induced charge transfer at graphene/TiO_x heterostructure interfaces. The breakthrough of discovering the sunlight-activated graphene-heterostructure transparent cathodes can be also applied in other photovoltaic systems which require a stable graphene-based transparent cathode consisting of low work function and excellent conductivity.